

Synthesis and characterization of spin-coatable *tert*-amine molecules for hole-transport in organic light-emitting diodes

A. Mishra,* P. K. Nayak, D. Ray, M. P. Patankar, K. L. Narasimhan and N. Periasamy*

Tata Institute of Fundamental Research, Homi Bhabha Road, Colaba, Mumbai 400 005, India

Received 13 December 2005; revised 18 April 2006; accepted 26 April 2006

Available online 19 May 2006

Abstract—The synthesis of two *tert*-amine-based, non-fluorescent, hole-transport molecules (4,4'-[bis-((4-di-*n*-hexylamino)benzylideneamino)]stilbene (**DHABS**) and 4,4'-[bis-((4-diphenylamino)benzylideneamino)]stilbene (**DPABS**) that are suitable for spin coating on indium tin oxide (ITO) for electronic device fabrication is described and compared with the widely used TPD. Electroluminescence occurred at a turn-on voltage of 7–8 V in ITO/hole-transport layer (HTL, spin coated)/Alq₃/Al devices. © 2006 Elsevier Ltd. All rights reserved.

Thin films of organic molecules and polymers can serve as semiconductors and are used in new generations of electronic devices such as field effect transistors and LEDs.^{1–3} Several *tert*-amine-based small molecules and polymers have been investigated for applications such as xerography and organic light-emitting diodes (OLEDs).^{4,5} For OLED devices, a few '*tert*-amine' molecules (*N,N'*-diphenyl-*N,N'*-bis(3-methylphenyl)-(1,1'-biphenyl)-4,4'-diamine (TPD) and *N,N'*-diphenyl-*N,N'*-bis(1-naphthyl)-(1,1'-biphenyl)-4,4'-diamine (NPB)) were found to be suitable for hole injection at the indium tin oxide electrode and efficient hole-transport with a field dependent hole mobility of $1\text{--}2 \times 10^{-3} \text{ cm}^2/\text{V s}$, and hence are widely used.⁶ The success stories of a few molecules have spurred synthetic activity in designing molecules which mimic the chemical structure of well-known molecules such as TPD and NPB, whilst expecting enhancement in desirable physical properties. TPD and NPB are sublimable and readily used to make devices by vapour deposition in conjunction with other small molecules such as, for example, tris(8-hydroxyquinolato)aluminium(III) (Alq₃). Recently, we synthesized a series of derivatives of Alq₃, which were based on modified 8-hydroxyquinol-

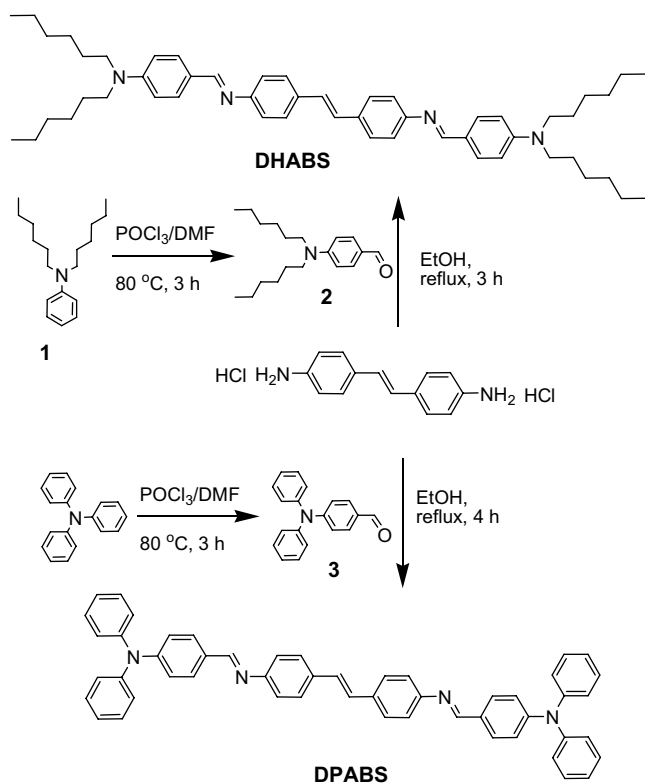
ine.^{7,8} These high-mass molecules were not sublimable but were soluble in organic solvents such as xylene. Organic devices can be made with these molecules only by using the technique of spin coating. Hole-transport molecules specifically suitable for spin coating have been reported,⁹ but are not yet commercially available. In this letter, we describe two hole-transport molecules that are suitable for spin coating for organic electronics.

N,N-Di-*n*-hexylaniline **1** prepared by reaction of aniline with 1-hexyl bromide, was formylated via a standard Vilsmeier reaction using DMF and phosphoryl chloride to give the aldehyde **2** as a colourless viscous liquid. 4-(Diphenylamino)benzaldehyde **3** was prepared via formylation of triphenylamine as a yellow solid in 72% yield.¹⁰ The compounds were characterized by ¹H NMR, ¹³C NMR, ESI-MS, and elemental analysis.¹¹ Condensation of aldehydes **2** and **3** with 4,4'-diaminostilbene dihydrochloride afforded 4,4'-[bis-((4-di-*n*-hexylamino)benzylideneamino)]stilbene (**DHABS**) and 4,4'-[bis-((4-diphenylamino)benzylideneamino)]stilbene (**DPABS**) as yellow crystalline solids (Scheme 1).¹²

Thin films of **DHABS** and **DPABS** on glass and UV-treated ITO substrates were prepared by spin coating using, after filtering through a 0.2 μm filter, solutions of 20 mg/mL of **DHABS** in xylene or 3.3 mg/mL of **DPABS** in chloroform, at 3000 rpm under a nitrogen atmosphere. The film thickness was directly determined by atomic force microscopy (AFM) after making a

Keywords: *tert*-Amine; OLED; Hole-transport layer (HTL); Electroluminescence; Spin coating.

*Corresponding authors. Fax: +91 22 22804610; e-mail addresses: peri@tifr.res.in; amaresh.mishra@rediffmail.com



Scheme 1. Synthesis of DHABS and DPABS.

scratch mark using a sharp blade which exposed the substrate. Using the absorbance of the film at λ_{\max} , the absorption coefficient was determined to be $1.56 \times 10^5 \text{ cm}^{-1}$ at 391 nm for **DHABS** and $1.24 \times 10^5 \text{ cm}^{-1}$ at 398 nm for **DPABS**. In a separate experiment, a film of thickness (t in Å) on the substrate of area (A in cm^2) was redissolved in chloroform (v in mL) and the absorbance (OD) of the solution was measured at λ_{\max} . The densities of the solid films of **DHABS** and **DPABS** were determined using the formula, $d \text{ (g/mL)} = 10^5 \text{ OD}vM/\varepsilon LA t$, where M is the molecular mass, ε is the molar extinction coefficient ($\text{M}^{-1} \text{ cm}^{-1}$) at λ_{\max} , L (cm) is the optical path length in the absorption measurement. The value of ε was $9.7 \times 10^4 \text{ M}^{-1} \text{ cm}^{-1}$ at 410 nm for **DHABS** in chloroform and $5.6 \times 10^4 \text{ M}^{-1} \text{ cm}^{-1}$ at 408 nm in chloroform for **DPABS**. The calculated density was 1.04 g/cc for **DHABS** and 1.42 g/cc for **DPABS**. The lower density is expected for **DHABS** because of the presence of an alkyl chain in the structure. The thickness of the spin coated layers of **DHABS** and **DPABS** on ITO was determined by capacitance measurements of ITO/**DHABS** (or **DPABS**)/Al devices, assuming that the dielectric constant of the organic materials was similar. The thickness measurement by capacitance was in agreement with the optical absorbance.

OLED devices were made by spin coating **DHABS** (or **DPABS**) on a pre-cleaned, pre-patterned ITO substrate followed by vacuum deposition of 600 Å Alq_3 , 10 Å LiF and an aluminium top contact through a metal mask. The depositions were carried out sequentially without breaking the vacuum. The thickness of the deposited

layers was monitored using a quartz crystal balance. The LiF layer was used to facilitate electron injection from the aluminium cathode. Some devices were made with PEDOT:PSS (Aldrich, USA) spin coated on ITO prior to spin coating the hole-transport layer. The typical device area was 1 mm^2 . Current–Voltage–Light (I – V – L) characteristics were measured in vacuum. Light measurements were made using a large area calibrated silicon photodetector placed in close proximity at a fixed geometry to the sample to collect the light through the substrate. The photodetector/geometry arrangement was calibrated to measure light emission from the device in Cd/m^2 . The thickness of the spin coated layers was measured using both optical absorption and capacitance measurements on the actual devices.

Figure 1 shows the absorption spectra of **DHABS** and **DPABS** in chloroform with λ_{\max} at 410 (**DHABS**) and 408 nm (**DPABS**). The spectra in thin film are similar, but the λ_{\max} is blue shifted by 19 nm (**DHABS**) and 12 nm (**DPABS**), respectively. The 0–0 transition corresponds to the crossing of the normalized absorption and emission spectra, which is 436 nm (2.84 eV) for **DHABS** and 439 nm (2.82 eV) for **DPABS**. Absorption spectra (transition energies) of **DHABS** and **DPABS** were also calculated by the quantum chemical method (MNDO/D) using HYPERCHEM software for a singly excited state up to 12 eV. The singlet excited state was calculated to be at 3.07 eV (401.5 nm) (**DHABS**) and 3.03 eV (406.9 nm) (**DPABS**), which did not match with the 0–0 transition. For comparison, the values for TPD were also determined by the same theoretical method which placed the singlet excited state at 3.2 eV (385.5 nm) which matched well with the 0–0 transition at 3.2 eV. We used the experimental values of the 0–0 transition energy for the placement of the lowest unoccupied molecular orbital (LUMO) level (see below) of **DHABS** and **DPABS**.

DHABS and **DPABS** are weakly fluorescent. The fluorescence quantum yields of **DHABS** and **DPABS** in chloroform were determined to be low with respect to

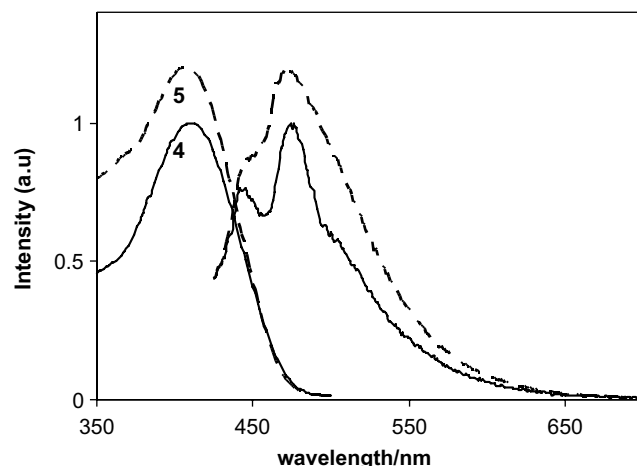


Figure 1. Absorption and emission spectra of **DHABS** (solid line) and **DPABS** (dashed line) in chloroform.

TPD in the same solvent. The ratio of the quantum yields is equal to the ratio of the area of the fluorescence spectra, corrected for the wavelength sensitivity of the photomultiplier, for samples of equal absorbance at the excitation wavelength. The quantum yield ratio was 0.036 for **DHABS** and 0.063 for **DPABS**, with respect to TPD.

The highest occupied molecular orbital (HOMO) levels of TPD, **DHABS** and **DPABS** were determined using cyclic voltammetry as follows. Current–voltage curves using Pt wire electrodes were obtained from solutions of the amine (TPD, **DHABS** or **DPABS**) and chloranil in dichloromethane with tetra-*n*-butylammonium fluoroborate (0.1 M) as the conducting salt. A complete cycle of potential sweep generates the reduction ($M \rightarrow M^-$) peak of chloranil and oxidation ($R \rightarrow R^+$) peak of the amine. The oxidation peaks of TPD, **DHABS** and **DPABS** were determined to be +0.70 V (TPD), +0.90 V (**DHABS**) and +0.54 V (**DPABS**) with respect to the reduction peak of chloranil. The reduction peak of chloranil with respect to the normal hydrogen electrode (NHE) occurs at +0.17 V. Thus, the oxidation potentials of the amines with respect to the NHE are +0.87 V (TPD), +1.07 V (**DHABS**) and +0.71 V (**DPABS**). The NHE level with respect to a vacuum is approximately -4.5 eV.^{1,13} Thus, the HOMO levels (i.e., the hole-transport levels) of the amines are located at -5.37 eV (TPD), -5.57 eV (**DHABS**) and -5.21 eV (**DPABS**). The LUMO levels (electron transport) are above the HOMO levels by the band gap energies which are the 0–0 transition energies determined from the absorption and emission spectra as above, which are 3.2 eV (TPD), 2.84 eV (**DHABS**) and 2.82 eV (**DPABS**). Thus the LUMO levels are at -2.17 eV (TPD), -2.73 eV (**DHABS**) and -2.39 eV (**DPABS**). It is to be noted that the HOMO–LUMO levels determined above are consistent with literature values for TPD within ± 0.2 eV.¹⁴ Thus, the values for **DHABS** and **DPABS** are expected to have the same uncertainty as that of TPD.

Figure 2 shows the energy levels of TPD, **DHABS** and **DPABS** together with those of ITO, Alq₃ and Al which

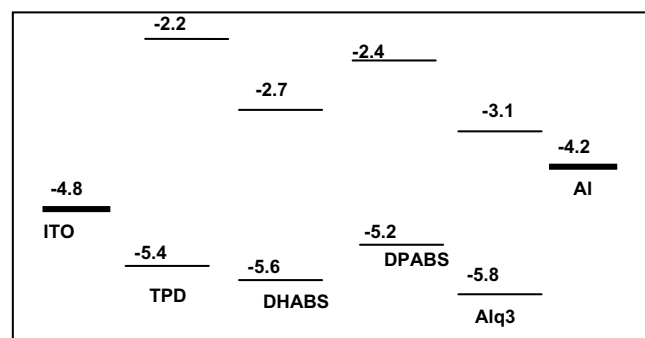


Figure 2. The Fermi level of ITO and aluminium electrodes and the HOMO–LUMO levels of the hole-transport *tert*-amine molecules (TPD, **DHABS** and **DPABS**) and the electron transport and luminescent molecule, Alq₃. The energy levels are given in eV with respect to the vacuum level as zero.

are used in the OLED structure. The HOMO level of TPD is at -5.4 eV, which means there is a barrier (0.6 eV) for hole injection from ITO. The HOMO levels of **DHABS** and **DPABS** indicate that the barrier is more (0.8 eV) and less (0.4 eV) by 0.2 eV for these molecules compared to TPD. OLED structures were made using Alq₃ as the electron transport layer (ETL). The existence of barriers for electrons and holes at the organic–organic interface has been shown to result in increasing of the efficiency of OLED devices.¹⁵ This condition is satisfied for TPD, **DHABS** or **DPABS** as HTL and Alq₃ as ETL. The HOMO and LUMO levels of Alq₃ are at -5.8 eV and -3.1 eV (see Fig. 2), which constitute an effective electron barrier from Alq₃ and hole barrier from the amine at the interface. Thus, based on energy level considerations, **DHABS** and **DPABS**, are expected to be suitable replacements for TPD.

The uniformity of the films of **DHABS** and **DPABS** on ITO was checked by AFM. The surface roughness (rms value) was estimated to be 4.7 nm (**DHABS**) and 1 nm (**DPABS**).

Four types of OLED devices were prepared, with and without PEDOT:PSS as a contact layer on ITO. These were ITO/**DHABS**/Alq₃/Al, ITO/PEDOT/**DHABS**/Alq₃/Al, ITO/**DPABS**/Alq₃/Al, and ITO/PEDOT/**DPABS**/Alq₃/Al. The thickness of the amine and Alq₃ layers were, 480 Å (**DHABS**) and 280 Å (**DPABS**) and 600–700 Å (Alq₃), respectively. The spin coating and other details (evaporation of Alq₃ film and metal film, encapsulation) are described above. The devices without PEDOT films gave better and more stable performance (current–voltage curves) than the devices containing PEDOT films. The results given below are for the devices without PEDOT films.

Figure 3 shows current as a function of applied bias voltage for the two devices. The figure shows that the current for the **DPABS** device is larger than that for **DHABS**. Figure 3 (middle panel) shows the EL–voltage characteristics for the same two devices. It is seen that the **DPABS** device exhibits better EL–voltage characteristics than the **DHABS** device. The voltage that marks the onset of EL for the **DPABS** device is lower (~ 7 V) than that for the **DHABS** device (~ 8 V). Figure 3 (bottom panel) shows the EL versus current (L – I) for the two devices. From the figure, the slope of the L – I curve is similar for the two devices at low current. Above 20 μ A, the **DPABS** device is much better.

As can be seen in Figure 2, the offset between the HOMO and the Fermi level of the ITO is smaller for **DPABS** (0.4 eV) than for **DHABS** (0.8 eV). The smaller barrier for hole injection should result in increased hole injection efficiency for the **DPABS** device. In fact, this barrier is even smaller than that for TPD (0.6 eV). We also see from the figure that the offset between the HOMO of Alq₃ and the HOMO of **DPABS** (0.6 eV) is larger than that for **DHABS** (0.2 eV). A large offset allows for holes to accumulate at the **DPABS**/Alq₃ interface and promote electron injection from the cathode. Both these features in the electronic energy levels

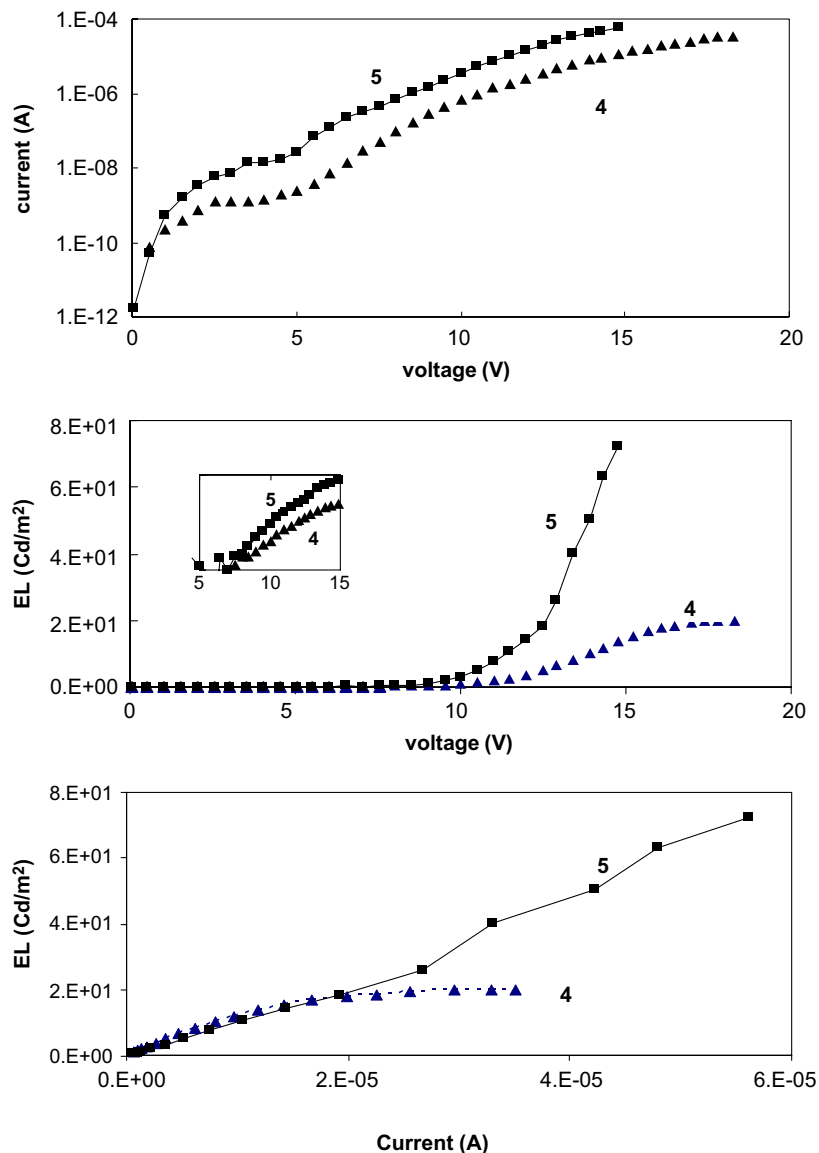


Figure 3. Current–voltage (top panel), EL intensity–voltage (middle) and EL–current (bottom) data for the OLED devices, ITO/DHABS (\blacktriangle)/Alq₃/Al and ITO/DPABS (\blacksquare)/Alq₃/Al. Inset in the middle panel shows EL versus voltage in log-linear scale, which shows the turn-on voltage at 8 and 7 V for DHABS and DPABS, respectively.

of DPABS vis-a-vis DHABS result in a lower turn-on voltage for the DPABS device and a larger forward bias current at a given voltage bias. It is interesting that the L – I characteristic is similar for the two devices at low current. At larger current (or voltage), the smaller L – I slope for DHABS suggests that the hole current leaks into the Alq₃ layer due to the low barrier of 0.2 eV and dominates the I – V characteristic. Thus, the L – I – V characteristics can be satisfactorily explained using the electronic levels of the molecules and the electrodes in OLED.

In conclusion, two spin-coatable hole-transport molecules (DHABS and DPABS) were synthesized which have HOMO levels comparable to the widely used TPD. OLED devices were made using a spin coated hole-transport layer and a vacuum evaporated electron transport layer (Alq₃) which showed EL at a turn-on

voltage of 7–8 V. The electroluminescence of the devices using spin-coated DHABS or DPABS as hole-transporters is weak compared to the standard devices using vacuum evaporated TPD as the hole-transporter. Spin coating and further processing of EL devices are still underway to improve the EL and current efficiency of these new compounds.

References and notes

1. Pope, M.; Swenberg, C. E. *Electronic Processes in Organic Crystals and Polymers*; Oxford University Press, 1999.
2. Kelley, T. W.; Baude, P. F.; Gerlach, C.; Ender, D. E.; Muires, D.; Haase, M. A.; Vogel, D. E.; Theiss, S. D. *Chem. Mater.* **2004**, *16*, 4413–4422.
3. Adachi, C.; Tsutsui, T. In *Organic Light Emitting Devices—A Survey*; Shinar, J., Ed.; Springer, 2002; Chapter 2; pp 43–69.

4. Tsutsui, T. *MRS Bull.* **1997**, *22*, 39–45.
5. Liu, S.; Jiang, X.; Ma, H.; Liu, M. S.; Jen, A. K. Y. *Macromolecules* **2000**, *33*, 3514–3517.
6. Stolka, M.; Yanus, J. F.; Pai, D. M. *J. Phys. Chem.* **1984**, *88*, 4707–4714.
7. Mishra, A.; Periasamy, N.; Patankar, M. P.; Narasimhan, K. L. *Dyes Pigm.* **2005**, *66*, 89–97.
8. Mishra, A.; Nayak, P. K.; Periasamy, N. *Tetrahedron Lett.* **2004**, *45*, 6265–6268.
9. Shirota, Y. *J. Mater. Chem.* **2000**, *10*, 1–25.
10. Baker, T. N.; Doherty, W. P.; Kelley, W. S.; Newmeyer, W.; Rogers, J. E.; Spalding, R. E. R.; Walter, I. *J. Org. Chem.* **1965**, *30*, 3714–3718.
11. *N,N-Di-n-hexylaniline* **1** was synthesized in 75% as a colourless viscous liquid; ^{13}C NMR (125 MHz, CDCl_3) δ 14.20 (CH_3), 22.80 (CH_3CH_2), 27.35, 28.20, 31.46 (CH_2), 51.38 (NCH_2), 114.29, 118.32, 129.70, 149.53 (C_{Ar}); ^1H NMR (500 MHz, CDCl_3) δ 0.94 (6H, t, $J = 6.4$ Hz, CH_3), 1.25–1.34 (12H, m, CH_2), 1.54 (4H, m, CH_2) 3.33 (4H, t, $J = 6.5$ Hz, CH_2), 6.60 (3H, m, ArH), 7.07 (2H, t, $J = 8.5$ Hz, ArH). Synthetic procedure for 4-(*N,N*-dihexylamino)benzaldehyde **2**: To a cooled (5 °C) solution of freshly distilled anhydrous DMF (20 g), was added POCl_3 (615 mg, 4 mmol) within 5 min. The mixture was stirred for 30 min, then **1** (1 g, 3.8 mmol) was added and the resulting mixture was heated for 3 h at 80 °C. The mixture was hydrolyzed by slow addition of ice-cold water and then neutralized with 5 M NaOH. The product was extracted with diethyl ether and washed with water and dried over MgSO_4 . After evaporation of the solvent in vacuo, the product was purified by column chromatography eluting with hexane–ethyl acetate (95:5) to afford the aldehyde **2** in 80% yield, as a viscous liquid: 885 mg; ^{13}C NMR (125 MHz, CDCl_3) δ 14.14 (CH_3), 22.80, 27.13, 28.10, 31.50 (CH_2), 51.39 (NCH_2), 114.79, 126.40, 130.78, 155.3 (C_{Ar}), 190.07 (CHO); ^1H NMR (500 MHz, CDCl_3) δ 0.90 (6H, t, $J = 6.43$ Hz, CH_3), 1.24–1.38 (12H, m, CH_2), 1.54 (4H, m, CH_2), 3.34 (4H, t, $J = 6.4$ Hz, CH_2), 6.76 (2H, d, $J = 9$ Hz, ArH) 7.62 (2H, d, $J = 9$ Hz, ArH), 9.85 (1H, s, CHO); ESI-MS m/z 290.3 ($\text{M}+\text{H}$) $^+$, 261.4 (M^+-CO), (Calcd for $\text{C}_{19}\text{H}_{31}\text{NO}$; 289.24).
12. General procedure for the synthesis of 4,4'-[bis-{(4-di-n-hexylamino)benzylideneamino}]stilbene (**DHABS**): To a solution of 4,4'-diaminostilbene dihydrochloride (200 mg, 0.7 mmol) in ethanol (10 mL) were added Et_3N (85.6 mg, 0.85 mmol) and **2** (430 mg, 1.49 mmol). The resulting mixture was stirred at reflux for 4 h. After cooling in an ice bath, the yellow precipitate formed was filtered and recrystallized from ethanol to afford **DHABS** in 92% yield, as a yellow solid: 489 mg; mp 160 °C. ^1H NMR (500 MHz, CDCl_3) δ 0.91 (12H, t, $J = 6.5$ Hz, CH_3), 1.31–1.40 (24H, m, CH_2), 1.51–1.70 (8H, m, CH_2), 3.33 (8H, t, $J = 7.5$ Hz, CH_2), 6.66 (4H, d, $J = 8.5$ Hz, ArH), 7.09 (2H, s, $\text{CH}=\text{CH}$), 7.19 (4H, d, $J = 8$ Hz, ArH), 7.52 (4H, d, $J = 8.5$ Hz, ArH), 7.73 (4H, d, $J = 8.5$ Hz), 8.33 (2H, s, $\text{CH}=\text{N}$); ESI-MS m/z 753.54 ($\text{M}+\text{H}$) $^+$, (Calcd for $\text{C}_{52}\text{H}_{72}\text{N}_4$; 752.58); Anal Calcd for $\text{C}_{52}\text{H}_{72}\text{N}_4$: C, 82.93; H, 9.64; N, 7.44; found: C, 83.05; H, 9.62; N, 7.58. 4,4'-[bis-{(4-diphenylamino)benzylideneamino}]stilbene (**DPABS**) was obtained in 92% yield as a yellow solid: mp 162 °C. ^1H NMR (500 MHz, CDCl_3) δ 6.67 (4H, d, $J = 8.5$ Hz, ArH), 6.84 (2H, s, $\text{CH}=\text{CH}$), 7.08–7.35 (24H, m, ArH), 7.33 (4H, d, $J = 8.5$ Hz, ArH), 7.74 (4H, d, $J = 8.5$ Hz), 8.40 (2H, s, $\text{CH}=\text{N}$); ESI-MS m/z 721.3 ($\text{M}+\text{H}$) $^+$, (Calcd $\text{C}_{52}\text{H}_{40}\text{N}_4$; 720.33); Anal Calcd for $\text{C}_{52}\text{H}_{40}\text{N}_4$: C, 86.64; H, 5.59; N, 7.77; found: C, 86.73; H, 5.54; N, 7.66.
13. This value of ~ 4.5 eV can be obtained using the thermodynamic data:

$\frac{1}{2}\text{H}_2(\text{g})$	\rightarrow	$\text{H}(\text{g})$,	$\Delta H = 2.25$ eV,
$\text{H}(\text{g})$	\rightarrow	$\text{H}^+(\text{g}) + \text{e}(\text{g})$,	$\Delta H = 13.6$ eV,
$\text{H}^+(\text{g})$	\rightarrow	$\text{H}^+(\text{aq})$,	$\Delta H = -11.3$ eV,
which give, $\frac{1}{2}\text{H}_2(\text{g}) \rightarrow \text{H}^+(\text{aq}) + \text{e}(\text{g}), \Delta H = 4.55$ eV.			
14. Shinar, J.; Savvateev, V. In *Organic Light Emitting Devices*; Shinar, J., Ed.; Springer: New York, 2004; p 15.
15. Brown, A. R.; Bradley, D. D. C.; Burroughes, J. H.; Friend, R. H.; Greenham, N. C.; Burn, P. L.; Holmes, A. B.; Kraft, A. *Appl. Phys. Lett.* **1992**, *61*, 2793–2795.